

# Robust Humanoid Walking on Compliant and Uneven Terrain with Deep Reinforcement Learning

Rohan P. Singh<sup>1,2</sup>, Mitsuharu Morisawa<sup>1</sup>, Mehdi Benallegue<sup>1</sup>,  
Zhaoming Xie<sup>3</sup>, Fumio Kanehiro<sup>1,2</sup>  
Email: rohan-singh@aist.go.jp

**Abstract**—For the deployment of legged robots in real-world environments, it is essential to develop robust locomotion control methods for challenging terrains that may exhibit unexpected deformability and irregularity. In this paper, we explore the application of *sim-to-real* deep reinforcement learning (RL) for the design of bipedal locomotion controllers for humanoid robots on compliant and uneven terrains. Our key contribution is to show that a simple training curriculum for exposing the RL agent to randomized terrains in simulation can achieve robust walking on a real humanoid robot using only proprioceptive feedback. We train an end-to-end bipedal locomotion policy using the proposed approach, and show extensive real-robot demonstration on the HRP-5P humanoid over several difficult terrains inside and outside the lab environment.

Further, we argue that the robustness of a bipedal walking policy can be improved if the robot is allowed to exhibit aperiodic motion with variable stepping frequency. We propose a new control policy to enable modification of the observed clock signal, leading to adaptive gait frequencies depending on the terrain and command velocity. Through simulation experiments, we show the effectiveness of this policy specifically for walking over challenging terrains by controlling swing and stance durations.

The code for training and evaluation is available online <sup>†</sup>.

## I. INTRODUCTION

Uncertainties in terrain properties — such as the height profile and deformability — present significant challenges for conventional model-based approaches to humanoid locomotion. This is primarily due to the strict temporal and spatial assumptions placed by such approaches on the foot trajectories and environmental contacts [1], [2]. When faced with an irregular or compliant (i.e. deformable) surface, these assumptions may be violated because of premature or delayed foot landing leading to negative consequences on the control. This is especially critical for humanoid robots with their large mass and bipedal support on bulky legs.

For real-world applications, it is important to develop a single, unified locomotion controller that can enable the robot to walk on different terrain types without the need for gait parameter tuning or manual specification of surface properties. Furthermore, as different terrains entail different walking strategies and contact timings [3], [4], the controller

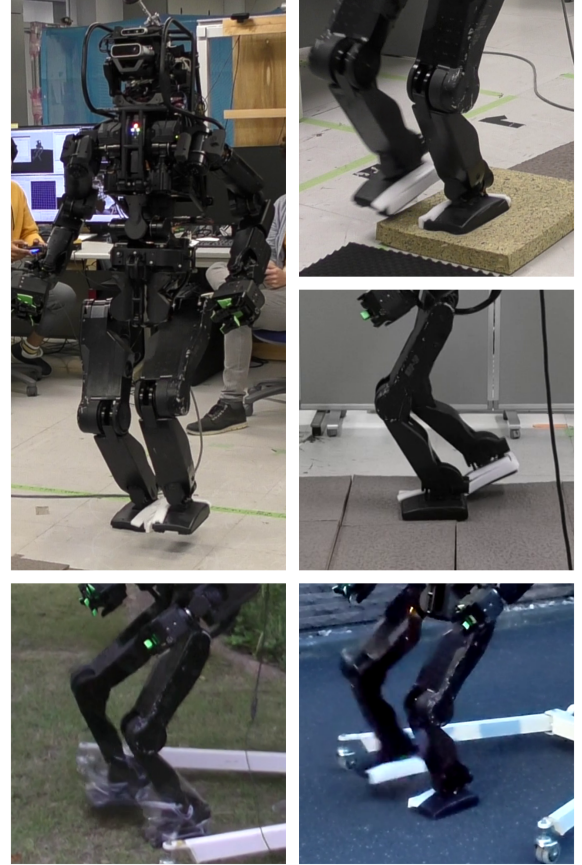


Fig. 1: **HRP-5P humanoid** bipedal locomotion (clockwise) on flat rigid floor, soft cushion, uneven inclined blocks, paved street, and grass using learned policy. The same RL policy was used for all terrains without any parameter tuning in between experiments. Lifter and overhead crane serve as a failsafe, the ropes are slack and robot is not provided external support.

must preferably be *adaptive* — to adapt the gait according to the type of terrain.

The problem becomes more complicated in the case of blind locomotion, that is, when the robot is unable to perceive the compliance and topography of the upcoming environment using exteroceptive sensors. In such cases, the controller needs to estimate the terrain properties from the observed state, more specifically, from joint positions and velocities, inertial measurement unit (IMU), clock signal, etc.

In this work, we present a locomotion controller for bipedal walking on deformable and uneven terrains using model-free deep RL without relying on explicit identification

<sup>1</sup> CNRS-AIST JRL (Joint Robotics Laboratory) IRL, National Institute of Advanced Industrial Science and Technology (AIST), Japan.

<sup>2</sup> University of Tsukuba, Ibaraki, Japan.

<sup>3</sup> Department of Computer Science, Stanford University, USA.

<sup>†</sup><https://github.com/rohanpsingh/LearningHumanoidWalking>

or classification. Instead, we let the controller learn to implicitly adapt to different terrains by exposing it to a range of terrains during the training phase in a simulation environment. By using a combination of one-hot representation of the user-commanded walking mode and clock-based reward terms [5], we propose to develop a single policy that can perform multiple *modes* of walking: stepping and turning in-place, walking forward, and quit standing.

Then, we perform *sim-to-real* transfer to deploy the trained policy on the real HRP-5P humanoid robot [6] on different types of environments, both indoors and outdoors.

Next, we propose to further enhance the robustness of the walking policy by learning policies that can predict clock signal modulations and achieve *aperiodic* gaits. Intuitively, these modulations further relax the constraints on the RL agent on contact timing, and consequently alleviate the challenge of premature and delayed landing of the swing foot on unknown terrains. We evaluate this policy systematically in the simulation environment and demonstrate the advantage of adaptive stepping frequency specifically for challenging terrain locomotion.

## II. RELATED WORKS

### A. Conventional approaches

Methods based on analytically-derived models of the robot locomotion dynamics have been used for humanoid locomotion, such as the linear inverted pendulum model [7] and its variants and the hybrid zero dynamics [8]. Both approaches have led to recent successful robust implementation on various kinds of terrains [9], [10].

An important work on the TORO robot [9] shows impressive locomotion over rough terrain, grass, and a soft gym mattress. However, like several other model-based methods, it involves manual tuning of gait parameters (timing, step length) and task gains.

Further work has been developed specifically to tackle terrains. For instance, some works have focussed on the optimization of gait parameters based on analysis of human experimental data [3], or based on terrain classification from tactile measurements [4]. Similarly, step adjustment based on divergent component of motion (DCM) error on a torque-controlled humanoid has been attempted [11]. Other works have been limited to the simulation environment, for ground reaction force (GRF) based control [12], and for simulation of sinkage phenomena on soft terrains [13].

A parallel approach has been to design new feet mechanisms for better passive and active terrain adaptation [14].

### B. Data-driven approaches

More recently, deep reinforcement learning (RL) has emerged as a radically new approach for legged locomotion. Application of deep RL to real quadrupedal robots has quickly equalled or surpassed model-based approaches in terms of locomotion performance in outdoor environments [15], [16], [17]. Bipedal locomotion has also been achieved with deep RL on lighter bipeds and humanoids like Cassie [18], [19] and Digit [20], [21], and on smaller humanoid

platforms [22], [23]. However, demonstrations on life-sized humanoids like the HRP-5P [24] and TOCABI [25] have mostly been confined to flat terrains with relatively small obstacle size.

Moreover, while demonstrations on rigid obstacles on stiff surfaces has been shown, learning-based approaches for compliant surfaces are more limited.

Note that the challenge posed by such terrains is especially greater for HRP-5P, compared to robots with lighter legs [15], [26]. During the training phase in simulation, due to the large inertia, low backdrivability, and low joint speeds, HRP-5P may find it much more difficult to recover from an unexpected collision with an obstacle — leading to degraded learning. This means that exploration during training can be problematic in an environment with large obstacles. On compliant surfaces, the surface will yield considerably more under the large total mass of HRP-5P.

Hence, the application of end-to-end deep RL policies for life-sized humanoids to tackle challenging terrains is a matter of investigation.

## III. ENVIRONMENT

We use model-free deep reinforcement learning to train our locomotion policies in a simulation environment, and provide the details of the RL environment in this section.

### A. Observations, Actions, and Rewards.

**Observation space.** Similar to [24], [27], the policy observation space includes the robot state and the external state (refer to Table I).

The robot state includes proprioceptive measurements from the encoders, on-board IMU, and motor current sensors. The current measurements are scaled to joint-level torque using the gear ratio and torque constant.

To control the robot's walking speed and direction, we use a 3D one-hot encoding to denote the walking mode —  $[0, 0, 1]$  for standing and  $[0, 1, 0]$  for stepping in-place and  $[1, 0, 0]$  for walking forward — and a 1D scalar to denote the reference value for the turning speed or the forward walking speed, depending on the mode. On the real robot, the values for the walking mode and mode reference are obtained from the robot operator using a joystick.

A clock signal is derived from a cyclic phase variable  $\phi$  as follows:

$$\text{clock} = \left\{ \sin\left(\frac{2\pi\phi}{L}\right), \cos\left(\frac{2\pi\phi}{L}\right) \right\}, \quad (1)$$

where  $L$  is the cycle period.  $\phi$  increments from 0 to 1 at each control timestep and reset to 0 after every  $L$  timesteps. Clock is then used as input to the policy. We set the gait cycle duration to 2 seconds (at 40Hz control frequency,  $L = 2 \times 40 = 80$  timesteps).

**Action space.** The 12D action space of the policy is comprised of the desired positions of the actuated joints of the robot's legs (6 in each). The predictions from the network are added to fixed motor offsets corresponding to a nominal

posture and are then tracked using a low-gain PD controller (see Table II):

$$\tau_{pd} = K_p(q_{des} - q) + K_d(0 - \dot{q}), \quad (2)$$

where  $K_p$  and  $K_d$  denote the proportional and derivative gain factors respectively.  $q_{des}$  is the policy prediction summed with the fixed motor offsets.  $q$  and  $\dot{q}$  denote the measured joint position and velocity. In the simulation environment, this torque drives the direct-drive motors while on the real robot, this is further tracked using low-level current controllers [23], [24]. The upperbody joints are frozen in the nominal configuration using stiff PD control. The policy is executed at 40Hz while the PD loop runs at 1000Hz, both in simulation and on real robot.

**Reward design.** We adopt the same reward function as in [24]. The full reward function consists of the bipedal gait terms inspired from previous works [28], [5], terms to encourage tracking of the walking mode command and reference speed, and terms for developing realistic motion for safer *sim-to-real* transfer. The terms are listed in Table III along with their relative weights. We refer the reader to [24] and the open-source code <sup>1</sup> for the precise description of each term.

### B. Initialization and Termination.

At the start of each training episode, the robot joints are initialized to the “half-sitting” posture (the configuration at which the robot can remain upright and prevent falling in the absence of external disturbances) injected with a small amount of noise <sup>2</sup>. The phase variable  $\phi$  is initialized to 0 and the walking mode is set to *Standing*.

Early termination conditions are needed to avoid exploration in irrecoverable states. We enforce a fall conditions, reached when the root height from the lowest point of foot-floor contact is less than 60cm, and a self-collision condition. An episode ends either after a fixed number of control timesteps or when a termination condition evaluates to true.

### C. Target terrains.

Our primary objective in this work is to enable the robot to walk successfully over terrains of different compliance, small inclines, rigid obstacles, and ground unevenness. For evaluating the real robot’s locomotion capabilities in indoor experiments, we created a testbed consisting of the following surfaces: a flat, stiff floor, a blue mattress, a block of soft cushion foam, rigid blocks of varying inclination, height and unevenness.

For evaluations in outdoor environments, we perform demonstrations in a grass lawn (deformable and with small obstacles) and paved street (gently inclined).

TABLE I: Policy Inputs.

	Observation	Dimension
Robot state	root orientation (roll, pitch)	2
	root angular velocity	3
	joint positions	12
	joint velocities	12
	motor currents	12
External state	Mode ( <i>Standing, Inplace, Forward</i> )	3
	Mode reference	1
	Clock	2

TABLE II: Policy Outputs.

	Action	Kp	Kd
Leg joints	(R/L) hip yaw	200	20
	(R/L) hip roll	150	15
	(R/L) hip pitch	200	20
	(R/L) knee pitch	150	15
	(R/L) ankle pitch	80	8
	(R/L) ankle roll	80	8

## IV. TRAINING FOR CHALLENGING TERRAINS

In this section, we first describe each of the key components of our pipeline for training a robust policy in MuJoCo and for achieving real robot deployment. Then, in section V, we introduce a new policy architecture that can predict clock signal modulations for aperiodic gait on challenging terrain.

### A. Simulating Compliance

We investigate how to simulate the foot sinking effect of walking on soft terrains in the MuJoCo simulation environment by exploiting the physics engine’s soft contact model. MuJoCo allows users to set the solver parameters for each constraint independently to achieve the desired behavior [29].

To this end, we adjust the *time constant* parameter of the mass-spring-damper model of the contact constraint between the feet and the ground bodies. We vary this parameter in the range of (0.02, 0.4) to simulate from a completely stiff to a more spring like behavior of the feet contact with the ground. Notably, we found that it is more convenient to set the *time constant* parameter for the robot’s feet “geoms” instead of the floor “geoms”, especially because we also modify the ground profile continuously during an episode to simulate an uneven terrain.

### B. Simulating Unevenness

A commonly used approach for learning robust legged locomotion is to train the policy in a simulation environment containing random discrete obstacles, slopes, and stairs. Here the agent acts blindly and effectively learns recovery strategies by making continual collisions with the environment, relying only on the proprioceptive state [15], [26]. However, as mentioned previously, blind locomotion in the presence of large obstacles may be infeasible for HRP-5P.

<sup>1</sup><https://github.com/rohanpsingh/LearningHumanoidWalking>

<sup>2</sup>Initialization noise was ultimately deemed to be unnecessary during real robot experiments.

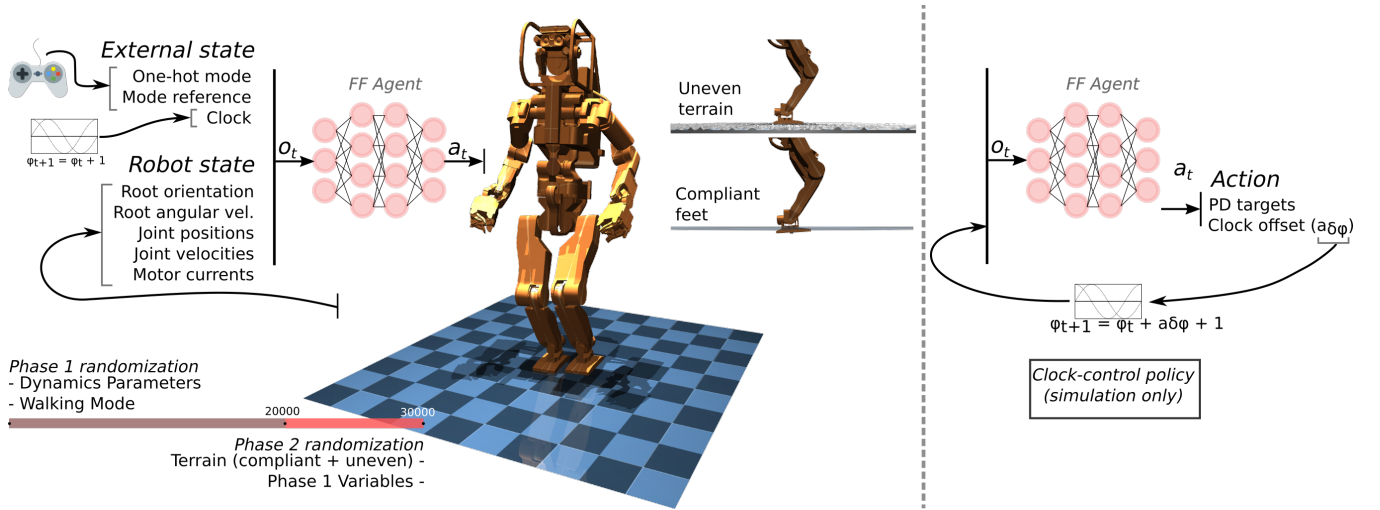


Fig. 2: **Overview of our training framework.** (L) We propose to train a feedforward RL agent while exposing it to randomized dynamics parameters in the first phase and then, additionally, randomized uneven and compliant terrains in the second phase. The policy achieves zero-shot *sim-to-real* transfer on the real HRP-5P. (R) We also propose an augmented policy that can make clock signal modifications for regulating the stepping frequency to achieve improved robustness on challenging terrains.

TABLE III: Reward Function.

	Term	Weight
Bipedal walking (clock-based)	Foot force	0.225
	Foot speed	0.225
Objective	Forward velocity	0.1
	Turning velocity	0.1
	Root height	0.05
Safety and Realism	Upper-body	0.1
	Nominal posture	0.1
	Joint velocities	0.1

In this work, we limit the peak height of obstacles on the floor to 4 cm during training. We simulate floor unevenness using the height fields functionality of MuJoCo. At the start of the training we generate one height field of size  $10m \times 10m$  and a grid size of 4 cm. This height field is placed along with the default rigid, flat floor. Then, during the training episodes, we randomize the  $z$  position of this height field relative to the flat floor. This creates the effect of generating a new terrain at each randomization with some obstacles of varying height scattered on a flat floor at irregular intervals. The  $z$ -position lies in the range of  $(-4 \text{ cm}, 0 \text{ cm})$ , creating a completely flat floor at  $z = -4 \text{ cm}$  and a fully uneven terrain (i.e. no flat regions) at  $z = 0 \text{ cm}$ . By pre-generating the height field in advance and randomizing its position, we eliminate the need to generate a new height field at each episode, saving valuable simulation time.

One limitation of this approach is that, during randomization of the terrain, the uneven floor may move under the support foot in such a way so as to produce an upward thrust. This is unlikely to happen in the real world. We mitigate this (partially) by disabling terrain unevenness randomization in double-support phase, that is, when both feet are on the ground.

### C. Curriculum Learning

Our training procedure is shown in Figure 2L. The training is done iteratively in two phases to achieve the final policy deployed on the real robot. First, we train a base policy for all walking modes on a flat, rigid floor. The walking modes are randomly switched between *Standing*, *Inplace*, *Forward* at every 5s in an episode. However, the switch into and out from *Standing* mode is allowed only when the clock signal is the double-support region. The mode reference value is simultaneously sampled at each switch from a uniform range of  $(-0.5, 0.5)\text{rad s}^{-1}$  turning speed if the mode is *Inplace* and a  $(0.1, 0.4)\text{m s}^{-1}$  forward walking speed if the mode is *Forward*.

In the second phase, we finetune the base policy for challenging terrain by initiating a new training process starting from the pre-trained network weights. The compliance of each foot (“solref” parameter in MuJoCo) is randomized after every 0.5s on average in the uniform range  $(0.02, 0.4)$  in an episode. The randomization range was determined through trial-and-error and visually inspecting the contact behavior of the simulated robot. The 3D position of the uneven terrain (simulated using “height fields” in MuJoCo) is randomized at every 5s interval on average and is disabled during double-support. The  $x, y$ - positions are sampled uniformly from the range  $(-0.5, 0.5)\text{m}$ , and  $z$ - position from  $(-0.04, 0)\text{m}$ . Walking mode randomization is continued as in the previous phase.

### D. Dynamics Randomization

We found that it is much more effective to randomize a small set of dynamics parameters of the robot model *during an episode* at some reasonable time interval, rather than at the start of the episode (conventional approach). This can be explained by the fact that our simulation environment is unable to model some aspects of the real robot dynamics realistically. For example, in the case of joint friction, natively

TABLE IV: Dynamics Randomization.

Parameter	Unit	Range
Joint damping coefficient	-	(0.2, 5)
Joint static friction	N – m	(2, 8)
Link mass	-	$[0.95, 1.05] \times \text{default}$
Link CoM ( $x, y, z$ )	m	$\pm 0.01$ from default

MuJoCo only allows us to simulate a simple friction model (dry and Coulomb friction), while the real joint friction displays a much more complex behavior. Thus, randomizing the friction coefficients during an episode will help prevent the agent from overfitting to one specific friction dynamics.

We sample a new set of dynamics parameters on an average at every 0.5s, which is shorter than the length of one swing phase. Details about the parameters and corresponding sampling ranges are provided in Table IV.

## V. APERIODIC WALKING

While the above mentioned modifications to the training environment are necessary for training a policy for walking on challenging terrains, a reward function based on a cyclic clock signal of constant period (Table III) limits the robot to a rigid stepping pattern. We argue that as a consequence of this fixed, periodic stepping pattern, the robot is unable to overcome terrain challenges that require large deviations from the prescribed swing and stance durations. Such contact-timing deviations break the periodicity of bipedal gait encoded in some form in most model-based and model-free approaches. In other words, a fixed, periodic gait pattern acts as a hindrance to achieving higher robustness.

We explore whether the control policy can be trained to achieve aperiodic walking gait patterns and whether these aperiodic gaits can lead to higher robustness on uneven terrain. To this end, we introduce a new policy that can predict clock signal modulations such that new gait patterns may *emerge* to adapt to different terrains and command velocities (see Figure 2R).

Besides controlling the actuated joints of the robot we augment the policy output to control the clock signal by predicting scalar offsets to the phase variable. Consequently, for this policy the action space  $A \in \mathbb{R}^{13}$ , and the phase variable is computed as,

$$\phi_{t+1} = \phi_t + \text{clip}(a_{\delta\phi}, -5, 5) + 1 \quad (3)$$

where, the phase offset action  $a_{\delta\phi}$  is clipped to a conservative range  $(-5, 5)$  timesteps. This range corresponds to a per-step maximum allowable offset of  $5 \times 0.025\text{s} = 0.125\text{s}$  at 40Hz control frequency.

This has been proposed previously for clock-based policies on bipeds, but it was found to have negligible impact on the robot’s performance [26]. However, we believe that such clock-control offers a clear advantage for walking over uneven terrains and provide simulation evaluations in subsection VI-C to study its impact.

## VI. EXPERIMENTS

### A. Implementation Details

**Training.** Our training hyperparameters are the same as [24]. Each episode rollout spans a maximum of 10s of simulated time, and may reset if a terminal condition is met. Training for 30000 iterations takes around 20 hours (on a AMD Ryzen Threadripper PRO 5975WX CPU with 32 cores and 64 threads) to collect a total of 380 million samples for learning the full task. Both the actor and critic policies are represented by MLP architectures to parameterize the policy and the value function in PPO [30]. Both MLP networks have 2 hidden layers of size 256 each and use *ReLU* activations.

**Inference.** The policy is wrapped in a C++ *mc-rtc*<sup>3</sup> controller and is evaluated in *mc-mujoco* [31] before deployment. Controller execution is on HRP-5P’s onboard control PC (Intel NUC5i7RYH i7-5557U CPU with 2 cores, Ubuntu 18.04 LTS PREEMPT-RT kernel). The inference is done at 40 Hz with the PD controller running at 1000 Hz.

The measured current feedback from the motors is fed to the control policy’s observation after transformation to the joint-level torque space. We refer the reader to [24] for more details about current feedback for improved *sim-to-real* transfer.

### B. Locomotion on Indoor and Outdoor terrains

We created several test terrains inside the lab consisting of rigid irregular blocks, a soft gym mattress, and a cushion foam block. From the 9 trials performed on the test terrains, the proposed policy could succeed to traverse in 6 trials, that is, a success rate of 67%. It is important to note the reason for the 3 failed cases. In the first case, the policy triggered a conservative safety implemented in the robot middleware due to excessive ankle motion. The safety limits were consequently relaxed. The other two failures occurred while standing on a slope or stepping over obstacles higher than 4cm.

We noticed that the policy is prone to failure typically when in standing mode (i.e. a very long double-support phase) with both feet on an inclined slope. We suspect that this happens because the change in robot state due to incline occurs gradually over time, and it becomes difficult for the policy to observe and compensate for this slow change. Note that the policy was not trained for such a scenario, hence, we believe terrain slope randomization at training time may resolve this issue. Similarly, the robot struggled to step over obstacles of height greater than 4cm, which is the maximum height of unevenness during policy training. Training for obstacle heights beyond 4cm in simulation should be straightforward but may raise risks of robot damage during *sim-to-real*.

In the outdoor tests, the robot could successfully traverse a distance of approximately 25m on a paved street, and 30m on an irregular grass lawn area. The lawn provided a combination of irregularity and compliance due to small

<sup>3</sup>[https://jrl-umi3218.github.io/mc\\_rtc/index.html](https://jrl-umi3218.github.io/mc_rtc/index.html)

mounds and depressions that was different from the test terrains available in the lab.

**Ablations.** We studied the importance of randomizing the terrain properties during training using simulated and real robot experiments by evaluating four policies:

- (a) *Baseline*: trained only on flat floor
- (b) *Uneven terrain*: baseline policy finetuned on uneven but rigid terrain
- (c) *Fixed compliance*: baseline policy finetuned on uneven terrain with fixed compliance (*solref* parameter is set to 0.4)
- (d) *Terrain-randomized*: baseline policy finetuned on uneven terrain with randomized compliance (*solref* is in range  $[0.02, 0.4]$ ).

Only the *baseline policy* is trained from scratch, for a total of 20000 training iterations (or about 250 millions samples). All the other policies are finetuned starting from the baseline for 10000 iterations.

Not surprisingly, the *baseline policy* trained for a flat floor was unable to cope with even a small height of unevenness in the simulation with a very short mean time before episode termination — 1.35 s for 2 cm and 5.6 s for 1 cm peak unevenness, averaged over 20 episodes in each case. We did not attempt to walk over obstacles or soft terrain on the real robot with this policy.

*Uneven terrain* policy could succeed to walk on small obstacles (3.5 cm) on the simulated and real robot in several trials. However, since it was only trained on a rigid floor, the robot failed to walk more than a few steps on the compliant terrain (soft blue mat) in 5/5 trials.

*Fixed compliance* policy could succeed to walk on 3.5 cm rigid obstacles and also on the compliant terrain. However, since this policy was trained without randomizing the “softness” of the floor, the real robot seemed to struggle to walk on the flat floor, and appeared to make redundant (and dangerous) ankle twist motions. We only performed one trial with this policy on the robot.

We achieved the best performance with the *Terrain-randomized* policy. The policy appeared to adapt the ankle motion depending on the compliance of the terrain while placing the foot horizontally on the flat floor. We performed indoor and outdoor tests using this policy, with success rate noted above.

### C. Effect of Predicting Clock

As described in section V, we propose to augment the control policy’s action space such that it is able predict delta modifications to the observed clock signal. We evaluate the behavior of the clock-control policy ( $A \in \mathbb{R}^{13}$ ) and compare it to the default policy ( $A \in \mathbb{R}^{12}$ ) that cannot control the clock. Both policies were trained for challenging terrain using the same routine of pre-training on regular train followed by finetuning on randomized compliant and uneven terrain.

First, we observed that the clock-control policy achieves a higher reward during training compared to the default policy. Figure 3a) shows the training reward curves averaged

over 3 experiments with different random seeds. This is in alignment to our expectations — the ability to adapt footstep timing under the presence of external disturbances provides greater flexibility from a control standpoint. This is better understood by analyzing the ground reaction force (GRF) profiles of the two policies (Figure 3b). We deployed a 60-second episode for stepping in-place with each policy and recorded the vertical GRF of both feet on the same randomized terrain in simulation. The clock-control policy appears to modulate the swing and support durations (regions of zero and non-zero force, respectively) of the gait while the default policy exhibits a nearly regular gait pattern.

Next, we record the value of the phase variable  $\phi_t$  and the policy’s phase offset action  $a_{\delta\phi}$  for simulated episodes on a regular, rigid terrain, for walking forward at command speed of  $0.4\text{m s}^{-1}$  and for stepping in-place (see Figure 4). In either walking mode, we noticed that the policy learned to speed up the clock (default gait cycle duration was 2s). The average gait cycle duration was 1.55 s walking forwards at  $0.4\text{m s}^{-1}$  (which includes accelerating from start) and 1.71 s while stepping in-place. This shows that the clock-control policy prefers a shorter gait cycle duration in general, and an even shorter duration for walking at higher speeds. Since a shorter gait cycle implies more frequent stepping, the policy’s behavior could be attributed to its increased ability react faster to disturbances. We also noticed that policy mainly makes positive corrections to the clock even though it is allowed to rewind the time.

The advantage of the clock-control policy specifically for locomotion over challenging terrain can also be observed in terms of success rate on different terrains. Table V lists the mean time before termination for both policies at increasing peak height of unevenness with randomized foot compliance. The mean values are computed over 100 simulation episodes in each case (800 episodes in total) with each episode having a maximum length of 10 s. Both policies were trained for a maximum unevenness height of 4 cm, and consequently, have similarly high success on 4 cm terrains. However, the clock-control policy outperforms the default policy when tested on terrains with higher unevenness.

**Limitations.** We observed that real robot deployment of the clock-control policy is significantly more difficult than the default policy (fixed clock). As this modification increases the unpredictability of the robot’s motion that requires implementation of additional safety measures, we skip the evaluations of the clock-control policy on the real hardware in this work. However, our preliminary investigations show that the *sim-to-real* gap may be higher for the clock-control policy than for the default policy. This could be due to poor system identification of the robot joints, leading to the policy’s inability to make fine adjustments to contact timings and durations on the real robot.

## VII. CONCLUSION

In this work, we explored the application of model-free deep reinforcement learning for developing humanoid locomotion controllers, specifically, for walking on challenging



TABLE V: Mean Episode Length on Challenging Terrain (10s max length)

Unevenness height(cm)	Default(s)	Clock-Control(s)
4	9.925	9.925
5	9.675	<b>9.725</b>
6	8.875	<b>9.525</b>
7	6.975	<b>8.4875</b>

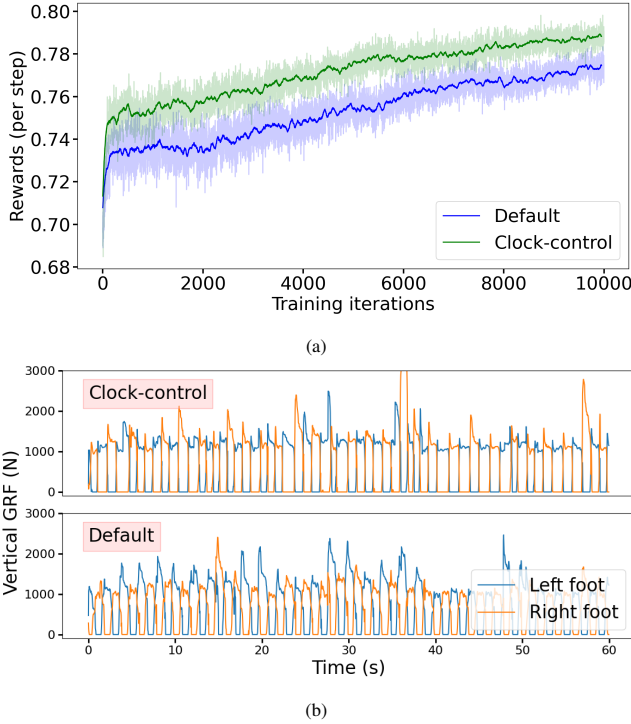


Fig. 3: **Behavior analysis of Clock Control (in simulation).** (a) Training reward curves for the clock-control policy and the default policy averaged over 3 training sessions with separate random seeds. Both policies are trained on randomized terrains starting from a regular terrain pre-trained policy. The clock-control policy converges to a higher reward. (b) 1-minute long episodes on the same uneven and soft terrain. The clock-control policy modifies the swing and stance duration in response to large disturbances while the default policy maintains a fixed gait pattern. **Note.** The sharp peak force for clock-control is due to inaccuracy in simulation (contact penetration).

terrains.

We showed that a relatively simple policy architecture and learning framework can attain promising locomotion performance on the real robot. In a simulation environment, we propose to first train a base policy on flat and rigid terrain, and then finetune the base policy on a uniformly randomized curriculum of compliant and uneven terrains. The RL agent comprises of a feedforward MLP network without incorporating observation history.

While it is difficult to quantitatively evaluate the wide range of existing humanoid locomotion controllers, in our experiments we found the proposed RL framework to have achieved remarkably robust locomotion performance. We were able to perform 2 outdoor experiments — without any falls in either trial or any other notable performance issues. Indoor locomotion over the soft cushion object also displayed

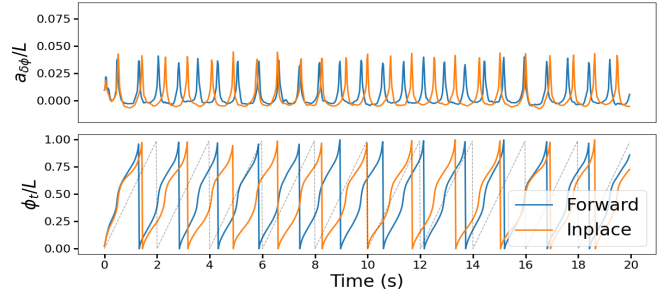


Fig. 4: **Evolution of the phase variable** for a 20-second episode rollout on flat, rigid terrain for walking forward and stepping in-place with a clock-control policy. Policy phase offset predictions (top) and the actual scalar phase variable (bottom) are both normalized by a fixed period  $L = 80$  for better visualization.

a robust success rate. Our real robot experiments also help validate the use of current feedback for achieving *sim-to-real* transfer [24] on the HRP-5P robot.

We also proposed a new method that can allow the policy to make modification to the observed clock signal. Through simulation experiments, we analyzed the behavior of this policy on different terrains and command velocities and observed the *emergence* of aperiodic gait patterns leading to improved locomotion robustness.

We release the source code on GitHub for simulating compliant and uneven terrain and for achieving omnidirectional walking behavior (with our existing RL training and evaluation framework) for better reproducibility of our work.

**Future work.** As the next step, we plan to deploy the clock-control policy on the real robot after introducing relevant safety measures and better system identification of the joint dynamics. We also hope to identify and overcome remaining factors for improving *sim-to-real* transfer such as link compliance and state estimation errors.

#### ACKNOWLEDGEMENTS

The authors thank all members of JRL for providing their support in conducting robot experiments that were done during the production of this work. This work was partially supported by JST SPRING Fellowship Program, Grant Number JPMJSP2124 and JSPS KAKENHI Grant Number JP22H05002.

#### REFERENCES

- [1] S. Kajita, M. Morisawa, K. Miura, S. Nakaoka, K. Harada, K. Kaneko, F. Kanehiro, and K. Yokoi, “Biped walking stabilization based on linear inverted pendulum tracking,” in *2010 IEEE/RSJ International Conference on Intelligent Robots and Systems*. IEEE, 2010, pp. 4489–4496.
- [2] S. Caron, A. Kheddar, and O. Tempier, “Stair climbing stabilization of the hrp-4 humanoid robot using whole-body admittance control,” in *2019 International Conference on Robotics and Automation (ICRA)*. IEEE, 2019, pp. 277–283.
- [3] K. Hashimoto, H.-j. Kang, M. Nakamura, E. Falotico, H.-o. Lim, A. Takanishi, C. Laschi, P. Dario, and A. Berthoz, “Realization of biped walking on soft ground with stabilization control based on gait analysis,” in *2012 IEEE/RSJ International Conference on Intelligent Robots and Systems*. IEEE, 2012, pp. 2064–2069.

- [4] K. Walas, D. Kanoulas, and P. Kryczka, "Terrain classification and locomotion parameters adaptation for humanoid robots using force/torque sensing," in *2016 IEEE-RAS 16th International Conference on Humanoid Robots (Humanoids)*. IEEE, 2016, pp. 133–140.
- [5] J. Siekmann, Y. Godse, A. Fern, and J. Hurst, "Sim-to-real learning of all common bipedal gaits via periodic reward composition," in *2021 IEEE International Conference on Robotics and Automation (ICRA)*. IEEE, 2021, pp. 7309–7315.
- [6] K. Kaneko, H. Kaminaga, T. Sakaguchi, S. Kajita, M. Morisawa, I. Kumagai, and F. Kanehiro, "Humanoid robot hrp-5p: An electrically actuated humanoid robot with high-power and wide-range joints," *IEEE Robotics and Automation Letters*, vol. 4, no. 2, pp. 1431–1438, 2019.
- [7] S. Kajita, F. Kanehiro, K. Kaneko, K. Fujiwara, K. Harada, K. Yokoi, and H. Hirukawa, "Biped walking pattern generation by using preview control of zero-moment point," in *2003 IEEE international conference on robotics and automation (Cat. No. 03CH37422)*, vol. 2. IEEE, 2003, pp. 1620–1626.
- [8] E. R. Westervelt, J. W. Grizzle, and D. E. Koditschek, "Hybrid zero dynamics of planar biped walkers," *IEEE transactions on automatic control*, vol. 48, no. 1, pp. 42–56, 2003.
- [9] G. Mesesan, J. Engelsberger, G. Garofalo, C. Ott, and A. Albu-Schäffer, "Dynamic walking on compliant and uneven terrain using dcm and passivity-based whole-body control," in *2019 IEEE-RAS 19th International Conference on Humanoid Robots (Humanoids)*. IEEE, 2019, pp. 25–32.
- [10] J. Reher and A. D. Ames, "Inverse dynamics control of compliant hybrid zero dynamic walking," in *2021 IEEE International Conference on Robotics and Automation (ICRA)*. IEEE, 2021, pp. 2040–2047.
- [11] M. A. Hopkins, R. J. Griffin, A. Leonessa, B. Y. Lattimer, and T. Furukawa, "Design of a compliant bipedal walking controller for the darpa robotics challenge," in *2015 IEEE-RAS 15th International Conference on Humanoid Robots (Humanoids)*. IEEE, 2015, pp. 831–837.
- [12] M. Komuta, Y. Abe, and S. Katsura, "Walking control of bipedal robot on soft ground considering ground reaction force," in *2017 IEEE/SICE International Symposium on System Integration (SII)*. IEEE, 2017, pp. 318–323.
- [13] S. Komizunai, A. Konno, S. Abiko, and M. Uchiyama, "Development of a static sinkage model for a biped robot on loose soil," in *2010 IEEE/SICE International Symposium on System Integration*. IEEE, 2010, pp. 61–66.
- [14] I. Frizza, H. Kaminaga, K. Ayusawa, P. Fraisse, and G. Venture, "A study on the benefits of using variable stiffness feet for humanoid walking on rough terrains," in *2022 IEEE-RAS 21st International Conference on Humanoid Robots (Humanoids)*. IEEE, 2022, pp. 427–434.
- [15] J. Lee, J. Hwangbo, L. Wellhausen, V. Koltun, and M. Hutter, "Learning quadrupedal locomotion over challenging terrain," *Science Robotics*, vol. 5, no. 47, 2020. [Online]. Available: <https://robotics.sciencemag.org/content/5/47/eabc5986>
- [16] T. Miki, J. Lee, J. Hwangbo, L. Wellhausen, V. Koltun, and M. Hutter, "Learning robust perceptive locomotion for quadrupedal robots in the wild," *Science Robotics*, vol. 7, no. 62, p. eabk2822, 2022.
- [17] S. Choi, G. Ji, J. Park, H. Kim, J. Mun, J. H. Lee, and J. Hwangbo, "Learning quadrupedal locomotion on deformable terrain," *Science Robotics*, vol. 8, no. 74, p. eade2256, 2023.
- [18] Z. Xie, P. Clary, J. Dao, P. Morais, J. Hurst, and M. van de Panne, "Learning locomotion skills for cassie: Iterative design and sim-to-real," in *Proc. Conference on Robot Learning (CORL 2019)*, 2019.
- [19] J. Siekmann, S. Valluri, J. Dao, L. Bermillo, H. Duan, A. Fern, and J. Hurst, "Learning memory-based control for human-scale bipedal locomotion," *arXiv preprint arXiv:2006.02402*, 2020.
- [20] L. Krishna, U. A. Mishra, G. A. Castillo, A. Hereid, and S. Kolathaya, "Learning linear policies for robust bipedal locomotion on terrains with varying slopes," in *2021 IEEE/RSJ International Conference on Intelligent Robots and Systems (IROS)*. IEEE, 2021, pp. 5159–5164.
- [21] I. Radosavovic, T. Xiao, B. Zhang, T. Darrell, J. Malik, and K. Sreenath, "Learning humanoid locomotion with transformers," *arXiv preprint arXiv:2303.03381*, 2023.
- [22] D. Rodriguez and S. Behnke, "Deepwalk: Omnidirectional bipedal gait by deep reinforcement learning," in *2021 IEEE international conference on robotics and automation (ICRA)*. IEEE, 2021, pp. 3033–3039.
- [23] S. Masuda and K. Takahashi, "Sim-to-real learning of robust compliant bipedal locomotion on torque sensor-less gear-driven humanoid," *arXiv preprint arXiv:2204.03897*, 2022.
- [24] R. P. Singh, Z. Xie, P. Gergondet, and F. Kanehiro, "Learning bipedal walking for humanoids with current feedback," *arXiv preprint arXiv:2303.03724*, 2023.
- [25] D. Kim, G. Berseth, M. Schwartz, and J. Park, "Torque-based deep reinforcement learning for task-and-robot agnostic learning on bipedal robots using sim-to-real transfer," *arXiv preprint arXiv:2304.09434*, 2023.
- [26] J. Siekmann, K. Green, J. Warila, A. Fern, and J. Hurst, "Blind bipedal stair traversal via sim-to-real reinforcement learning," *arXiv preprint arXiv:2105.08328*, 2021.
- [27] R. P. Singh, M. Benallegue, M. Morisawa, R. Cisneros, and F. Kanehiro, "Learning bipedal walking on planned footsteps for humanoid robots," in *2022 IEEE-RAS 21st International Conference on Humanoid Robots (Humanoids)*. IEEE, 2022, pp. 686–693.
- [28] C. Yang, K. Yuan, S. Heng, T. Komura, and Z. Li, "Learning natural locomotion behaviors for humanoid robots using human bias," *IEEE Robotics and Automation Letters*, vol. 5, no. 2, pp. 2610–2617, 2020.
- [29] E. Todorov, T. Erez, and Y. Tassa, "Mujoco: A physics engine for model-based control," in *2012 IEEE/RSJ international conference on intelligent robots and systems*. IEEE, 2012, pp. 5026–5033.
- [30] J. Schulman, F. Wolski, P. Dhariwal, A. Radford, and O. Klimov, "Proximal policy optimization algorithms," *arXiv preprint arXiv:1707.06347*, 2017.
- [31] R. P. Singh, P. Gergondet, and F. Kanehiro, "mc-mujoco: Simulating articulated robots with fsm controllers in mujoco," in *2023 IEEE/SICE International Symposium on System Integration (SII)*. IEEE, 2023, pp. 1–5.